Title

Crystallization of proteins from crude bovine rod outer segments.

Authors

Baker, Bo
Gulati, Sahil
Shi, Wuxian
et al.

Publication Date

2015

DOI

10.1016/bs.mie.2014.11.045

Peer reviewed

HHS Public Access

Author manuscript

Methods Enzymol. Author manuscript; available in PMC 2015 June 30.

Published in final edited form as:

Methods Enzymol. 2015 ; 557: 439–458. doi:10.1016/bs.mie.2014.11.045.

Crystallization of Proteins from Crude Bovine Rod Outer Segments☆

Bo Y. Baker[*,†,1], **Sahil Gulati**[*,†], **Wuxian Shi**[‡], **Benlian Wang**[‡], **Phoebe L. Stewart**[*,†], and **Krzysztof Palczewski**[*,†,1]

[*]Department of Pharmacology, Case Western Reserve University, Cleveland, Ohio, USA

[†]Cleveland Center for Membrane and Structural Biology, School of Medicine, Case Western Reserve University, Cleveland, Ohio, USA

[‡]Center for Proteomics and Bioinformatics, Center for Synchrotron Biosciences, School of Medicine, Case Western Reserve University, Cleveland, Ohio, USA

Abstract

Obtaining protein crystals suitable for X-ray diffraction studies comprises the greatest challenge in the determination of protein crystal structures, especially for membrane proteins and protein complexes. Although high purity has been broadly accepted as one of the most significant requirements for protein crystallization, a recent study of the *Escherichia coli* proteome showed that many proteins have an inherent propensity to crystallize and do not require a highly homogeneous sample (Totir et al., 2012). As exemplified by RPE65 (Kiser, Golczak, Lodowski, Chance, & Palczewski, 2009), there also are cases of mammalian proteins crystallized from less purified samples. To test whether this phenomenon can be applied more broadly to the study of proteins from higher organisms, we investigated the protein crystallization profile of bovine rod outer segment (ROS) crude extracts. Interestingly, multiple protein crystals readily formed from such extracts, some of them diffracting to high resolution that allowed structural determination. A total of seven proteins were crystallized, one of which was a membrane protein. Successful crystallization of proteins from heterogeneous ROS extracts demonstrates that many mammalian proteins also have an intrinsic propensity to crystallize from complex biological mixtures. By providing an alternative approach to heterologous expression to achieve crystallization, this strategy could be useful for proteins and complexes that are difficult to purify or obtain by recombinant techniques.

1. INTRODUCTION

While structural studies provide valuable information needed to understand physiological processes at the molecular level, X-ray crystallography has been the leading approach to determine protein structures at the atomic level. As of March 2014, the number of protein structures solved by X-ray diffraction methods reached 87,945, accounting for ~88.9% of

☆The structures reported in this study have been deposited in the Protein Data Bank (PDB) under accession codes 4O63 (bovine GAPDH_3NAD) and 4Q2R (bovine CK-B).

[1]Corresponding authors: byb@case.edu; kxp65@case.edu.

the total protein structures in the Protein Data Bank (PDB). Growing protein crystals suitable for X-ray diffraction studies comprises the major bottleneck in the process of solving a protein structure, especially for membrane proteins and protein complexes because variations in the molecular properties of each protein require specific crystallization conditions.

High purity of a protein sample has been broadly accepted as one of the most important requirements for crystallization. However, it is also well documented that protein crystallization can be used effectively for protein purification. Examples of proteins for which crystallization was used to obtain the highest level of purity include glycogen phosphorylase (Fischer & Krebs, 1958), cytochrome c2 (Pettigrew, Bartsch, Meyer, & Kamen, 1978), and lysozyme (Judge, Forsythe, & Pusey, 1998). Several unsuccessful protein complex crystallization attempts have still resulted in the crystallization of a single-protein component. Quite recently, the structure of bovine arrestin-1 splice variant (p^{44}) was determined from a mixture of arrestin with opsin (Kim et al., 2013). Though this co-crystallization failed, investigators were able to obtain crystals of the arrestin variant.

Several groups have studied the effect of impurities on protein crystallization. In 1998, Judge et al. investigated the effect of protein impurities on the crystallization of lysozyme from fresh chicken egg whites. Other proteins did not affect lysozyme crystal face growth even at concentrations of up to 50% of total protein in the sample (Judge et al., 1998). In 2006, Dong et al. reported an increase in the number of proteins forming diffraction-quality crystals upon addition of trace amounts of protease (Dong et al., 2007). The authors found that despite the presence of protease as well as cleaved peptides and protein fragments in these samples, protein crystals still formed readily, suggesting a certain tolerance for sample impurities during crystallization. Indeed, the presence of protease helped to remove flexible regions of target proteins and generated protein domains that improved crystallization.

Membrane proteins, particularly those derived from a vertebrate source/genome, pose a more difficult problem (Muller, Wu, & Palczewski, 2008). Certain properties of membrane proteins, including their hydrophobic nature, propensity to bind other hydrophobic partners in heterogeneous complexes, instability in detergents required for purification, conformational heterogeneity, and flexibility often constitute major obstacles for accurate structural and functional studies. In studying the effect of sample purity on membrane protein crystallization, Kors et al. (2009) discovered that a membrane protein, photosynthetic reaction center from *Rhodobacter sphaeroides*, produced crystals in the presence of substantial amounts of impurities (Kors et al., 2009). Unexpectedly, crystals were obtained with a protein/contaminant ratio as high as 50%, including lipid material and membrane fragments. In 2012, Alber's group investigated a native source of proteins for high-throughput protein crystallography applications (Totir et al., 2012). The authors separated 408 unique fractions from the *E. coli* proteome with protein purities ranging from 95% to less than 5%. Despite different levels of sample complexity, the authors were able to obtain crystals from 295 of these fractions, representing 73% of the total protein (Totir et al., 2012). This suggests that many proteins, if not all, have an inherent propensity to crystallize, even from samples of varying heterogeneity.

Mammalian proteins differ from bacterial proteins in several respects. During biosynthesis, mammalian proteins undergo various posttranslational modifications, such as phosphorylation for signal transduction and glycosylation needed for protein folding, distribution, and activity. Whether the findings discussed above apply more generally to proteins from higher organisms has not been established. Here, we used crude extracts from bovine rod outer segment (ROS) to investigate the potential of mammalian proteins from a native source to form crystals suitable for structural determination. ROSs are compartments of vertebrate rod photoreceptor cells in the eye's retina that are essential for visual phototransduction. The proteome of ROS contains about 516 proteins involved in transduction of visual signals, maintenance of retinal structure, and metabolic pathways (Kwok, Holopainen, Molday, Foster, & Molday, 2008), whereas the internal disc membranes are likely to have less than a dozen proteins (Skiba et al., 2013). Some proteins, such as the phosphodiesterase 6 (PDE6) heterotetramer and the transducin (G_t) heterotrimer complex are difficult to obtain by recombinant expression methods. Because of their high abundance in ROS, PDE6, and G_t are routinely purified from these compartments for biochemical and structural studies (Baker & Palczewski, 2011; Goc et al., 2008).

Here, we investigated the crystallization profiles of seven proteins from bovine ROS using a general screening approach. This study is the first attempt to crystallize mammalian proteins from a native source under highly heterogeneous conditions. The results provide an alternative approach to achieving crystallization of proteins that resist expression and purification or display conformational heterogeneity due to diverse folding. This study provides a powerful addition to current structural genomics initiatives by circumventing the need to attain homogeneity for protein crystallization.

2. EXPERIMENTAL PROCEDURES

2.1. Protein sample preparation

ROS membranes were isolated from 300 frozen bovine retinas (W. L. Lawson Co., Lincoln, NE) under dim red light as previously described (Baker & Palczewski, 2011). Soluble proteins were extracted from isolated ROS membranes three times with isotonic buffer containing 20 m*M* 2-[4-(2-hydroxyethyl)piperazin-1-yl]ethanesulfonic acid (HEPES), pH 7.5, 0.1 *M* NaCl, and 5 m*M* $MgCl_2$. Soluble protein extracts were combined and centrifuged at 30,940 × *g* for 30 min at 4 °C. The supernatant was further centrifuged at 30,940 × *g* at 4 °C for 50 min to remove any traces of membranes and dialyzed overnight at 4 °C against buffer containing 20 m*M* HEPES, pH 7.5. The dialyzed sample (named F_A) was used directly for crystallization screening or subjected to weak ion exchange chromatography on a 5 ml HiTrap Fast Flow DEAE Sepharose column (GE Healthcare BioSciences Corp, Piscataway, NJ) at a flow rate of 1 ml/min. The column was washed with 200 ml of buffer containing 20 m*M* HEPES, pH 7.5, and bound proteins were eluted by a linear NaCl gradient from 0 to 1 *M* over 120 ml at a flow rate of 1 ml/min. Fractions were collected for each of the eluted peaks and retained for further processing.

To separate glyceraldehyde 3-phosphate dehydrogenase (GAPDH), the flow-through (named F_B) from the diethylaminoethyl (DEAE)-Sepharose column was loaded onto a nicotinamide adenine dinucleotide (NAD)-agarose (Bio-WORLD, Dublin, OH) column. In

preparation, lyophilized NAD-agarose (1 g) was solubilized in water and packed into an Econo-Column (0.5 × 5 cm, BioRad, Hercules, CA). Before protein loading, the column was equilibrated with binding buffer (20 m*M* HEPES, pH 7.3). Protein samples were loaded onto the column at flow rate of 1 ml/min. The column was washed with 200 ml of binding buffer followed by elution of GAPDH with the elution buffer (20 m*M* HEPES, pH 7.3, 5 m*M* NAD). GAPDH was concentrated to 2–3 mg/ml prior to crystallization trials.

To separate arrestin-1, a method described previously (Buczylko & Palczewski, 1993) was used with a few alterations. Combined fractions of elution peak 1 (P1, named F_C) from the DEAE-cellulose column were dialyzed against buffer containing 20 m*M* HEPES, pH 7.3, and 0.1 *M* NaCl at 4 °C. The dialyzed sample was incubated with 4 ml (dry volume) of Heparin-Sepharose (GE Healthcare) for 3 h. The formed slurry was loaded onto a 1 × 7.5 cm Econo-Column (BioRad, Hercules, CA) and washed with 100 ml of loading buffer (20 m*M* HEPES, pH 7.3, 0.1 *M* NaCl). Arrestin-1 was eluted with elution buffer (20 m*M* HEPES, pH 7.3, 0.4 *M* NaCl), concentrated to ~5 mg/ml, and used for crystallization trials. Arrestin-1 was exclusively crystallized from F_C. The flow-through from Heparin-Sepharose (named F_G) was collected and dialyzed against 20 m*M* HEPES, pH 7.3, 0.1 *M* NaCl. The F_G was concentrated to ~10 mg/ml prior to crystallization trials. LDH crystals were grown from F_G.

Opsin was obtained from bovine ROS as previously described (Sachs, Maretzki, & Hofmann, 2000). Briefly, a ROS pellet was resuspended in buffer containing 10 m*M* sodium phosphate, pH 7.0, and 50 m*M* hydroxylamine. The ROS suspension was kept on ice and photobleached for 30 min under a 60-W incandescent white light bulb. The photobleached suspension then was centrifuged at 16,110 × *g* for 10 min at 4 °C, and the pellet was resuspended in 1 ml of solution containing 10 m*M* sodium phosphate, pH 6.5, and 2% bovine serum albumin (BSA). To remove hydroxylamine, the suspension was centrifuged again at 16,110 × *g* for 10 min at 4 °C, and the pellet was washed five times with BSA solution. In the last step, BSA was removed by washing the pellet six times with 1 ml of 10 m*M* sodium phosphate, pH 6.5. The resulting pellet containing opsin membranes was solubilized with 1 ml of solution containing 20 m*M* Bis-Tris-propane, pH 7.5, 130 m*M* NaCl, 1 m*M* $MgCl_2$, 10% sucrose, and 1% β-D-octylglucopyranoside for 1 h at room temperature. Insoluble material was removed by centrifugation at 16,110 × *g* for 5 min at 4 °C. Solubilized opsin then was concentrated to ~5 mg/ml with a 50 kDa cutoff Amicon Ultra-0.5 concentrator (Millipore, Billerica, MA) and used for crystallization.

2.2. Protein crystallization and validation

Crystallization trials were performed by the sitting-drop vapor-diffusion method. All screens were set up in 96-well plates with a Phoenix crystallization robot (Art Robbins Instruments, Sunnyvale, CA) (Mcpherson, 1991). Initial screenings were carried out with commercially available kits, included polyethylene glycol (PEG)/Ion, PEG/Ion2, and PEG/Rx Index from Hampton Research (Aliso Viejo, CA); AmSO4 Suite, JCSG+ Suite, and Protein Complex Suite from Qiagen (Valencia, CA); and Wizard from Emerald Bio (Bainbridge Island, WA). Plates were incubated at 4 °C or RT, and checked on a regular basis at least once every week for the first month and once per month thereafter. Once crystals (or “hits”) were observed,

experiments were repeated with minor optimizations such as varying the type and concentration of precipitant, pH, and temperature along with the mode of vapor diffusion (sitting or hanging drops).

Crystals were obtained by mixing equal volumes (150 nl) of protein and reservoir solution in 96-well plates (Intelli-Plate 96–2, Art Robbins, Sunnyvale, CA). GAPDH crystals formed in over 10 conditions from PEG/Ion screen kits, including conditions No. 2, 6, 21, 22, 23, and 27 from PEG/Ion and conditions No. 6, 14, 20, 40, and 46 from PEG/Ion 2. LDH crystals formed in 10% PEG 3.5 K, 0.1 *M* $MgSO_4$ from a custom-designed screen kit. Arrestin-1 crystals were found in over five conditions from PEG/Ion screen kits, including conditions No. 3, 5, 13, 25, and 29 from PEG/Ion 2. The majority of protein crystals in this study grew after incubation for 1–2 weeks at 4 °C with protein sample buffer containing 20 m*M* HEPES, pH 7.3, and 0.1 *M* NaCl. GAPDH crystals grew at 4 °C with a reservoir solution containing 20% PEG 3.5 K, 0.2 *M* succinic acid, pH 7.0. Diffraction-suitable LDH crystals grew at room temperature with a reservoir solution containing 10% PEG 3.5 K, 0.2 *M* sodium acetate. Arrestin-1 crystals grew at 4 °C with a reservoir solution containing 7.5% PEG 3.5 K, 0.1 *M* sodium malonate, pH 5.0, and 4% PEG 400.

Opsin crystals were obtained by hanging drop vapor diffusion after mixing equal volumes of protein at 5 mg/ml and the reservoir solution described above. Crystals reached their full size within 25 days at 4 °C. Prior to freezing in liquid nitrogen, crystals were soaked in their respective reservoir solutions supplemented with 10% glycerol. After X-ray diffraction experiments, single crystals were dissolved, and the proteins were separated with SDS-PAGE followed by silver staining.

2.3. Mass spectrometry analysis

Crystals (5–10 for each protein) were washed and analyzed by SDS-PAGE. Coomassie-stained SDS-PAGE bands were excised and bleached in a solution of 50 m*M* ammonium bicarbonate in 50% acetonitrile. Bands were dehydrated in 100% acetonitrile and dried in a Speedvac centrifuge. Prior to overnight in-gel trypsin digestion, thiol groups were reduced with 20 m*M* dithiothreitol at room temperature for 1 h, followed by alkylation with 50 m*M* iodoacetamide in 50 m*M* ammonium bicarbonate for 30 min in the dark. Proteolytic peptides were extracted from gels with 50% acetonitrile in 5% formic acid and then resuspended in 0.1% formic acid after being completely dried under vacuum. Analyses of the resulting peptides were performed with an Orbitrap Elite Hybrid Mass Spectrometer (Thermo Electron, San Jose, CA, USA) equipped with a Waters nanoAcquity UPLC system (Waters, Taunton, MA, USA). Spectra were recorded by data-dependent methods with an alternating full scan followed by 20 MS/MS scans. Obtained data were analyzed using Mascot Daemon (Matrix Science, Boston, MA), with the settings of : 10 ppm for parent ions and 0.8 Da for product ions. Carbamidomethylation of Cys residues was set as a fixed modification, and oxidation of Met residues as a variable modification.

2.4. Data collection and structural determination

Preliminary diffraction was tested with a Rigaku MicroMax-007HF in-house X-ray source. Higher resolution data were collected with synchrotron sources at beamline X29 of

Brookhaven National Laboratory (BNL) and NETCAT-24-ID-C at the Advanced Photon Source (APS), Argonne National Laboratory. Diffraction datasets were processed and scaled with HKL2000 (Otwinowski & Minor, 1997) and XDS (Kabsch, 2010a, 2010b). Protein structures were determined with the CCP4 suite version 6.4.0 (Winn et al., 2011) by molecular replacement with closely related homolog structures used as search models. Structures were refined by alternate rounds of manual rebuilding with COOT version 0.7.2 (Emsley, Lohkamp, Scott, & Cowtan, 2010) and automated refinement by REFMAC (Vagin et al., 2004). Figures were prepared with Chimera-1.8.1-win64 (Goddard, Huang, & Ferrin, 2007; Pettersen et al., 2004).

3. PILOT EXPERIMENTAL RESULTS

Isolation of ROS from bovine retinas was followed by isotonic extraction of proteins and DEAE-cellulose chromatography to enrich some proteins and prevent disruption of protein complexes, especially those with transient interactions. Unlike other proteins, opsin preparation from bovine ROS did not require further downstream treatment of ROS membranes. The overall experimental design is illustrated in Fig. 1.

Isotonic extracts of ROS (named F_A) obtained from 300 bovine retinas yielded ~20 mg of total protein. Fractionation of F_A extracts by DEAE-cellulose chromatography yielded three major peaks (Fig. 2A). Fractions from these peaks were collected along with the flow-through and analyzed by SDS-PAGE (Fig. 2B). All fractions were subsequently buffer exchanged by dialysis and concentrated prior to crystallization screening.

3.1. Protein crystals readily formed from ROS extracts

Initial screening of F_A extracts yielded more than 10 different types of crystals with various morphologies, including needles and thin rods. Subsequent SDS-PAGE and diffraction analysis of these crystals revealed that they all belonged to a single protein. Mass spectroscopy (MS) analysis identified this protein as GAPDH, a key enzyme involved in glycolysis. Because its high propensity to crystallize complicated our screening results and could have prevented crystallization of other proteins, the F_A fraction was subjected to DEAE-ion-exchange chromatography.

The DEAE-cellulose chromatography step added two benefits to sample preparation; it removed GAPDH from the F_A extract and increased the yield of less abundant proteins. However, using DEAE-cellulose chromatography has some drawbacks. This step could disturb interactions of weakly bound protein complexes in the F_A extract. GAPDH did not bind to the DEAE column and remained in the flow-through, from which it was recovered by affinity binding to a NAD-agarose column. The flow-through from NAD-agarose (named F_F) was collected, dialyzed against 20 m*M* HEPES, pH 7.3, 0.1 *M* NaCl, and concentrated to ~10 mg/ml for crystallization. Two proteins were crystallized from F_F, namely enolase and malate dehydrogenase. Enolase crystals grew in a reservoir containing 20% PEG 3.5 K and 0.2 *M* sodium thiocyanate. Maltase crystals were grown in 25% PEG 1 K, 0.1 *M* Na/K-phosphate, pH 6.5, and 0.2 *M* NaCl.

Bovine GAPDH crystals diffracted to ~2 Å as illustrated in Fig. 3A. The structure was determined by molecular replacement using the rabbit GAPDH structure (PDB ID: 1J0X) as the search model (Fig. 4A). The R_{work} and R_{free} of the final structure were 19% and 24%, respectively. Unit cell dimensions were a = 79.8 Å, b = 126.5 Å, c = 83.8 Å; α = 90°, β = 118°, γ =90°. Although bovine GAPDH existed as a homotetramer identical to known structures in this protein family, it had three NAD molecules bound instead of either two or four found in other mammalian GAPDHs, a feature that distinguishes it from others PDB entries, 1J0X (Cowan-Jacob, Kaufmann, Anselmo, Stark, & Grutter, 2003), 1U8F (Jenkins & Tanner, 2006), and 1ZNQ (Baker, Shi, Wang, & Palczewski, 2014).

Sparse-matrix commercial screening kits are designed to accommodate a broad range of conditions for crystallization of various proteins. However, these kits may not suffice for each individual protein. To establish crystallization conditions for interesting proteins in crude ROS extracts, we referred to the ROS proteome database (Kwok et al., 2008) and selected several groups of proteins as test targets. These were L-lactate dehydrogenase (LDH), macrophage migration inhibitory factor, creatine kinase-B type (CK-B), dynamin, pyrophosphatase, phosphofructokinase, T-complex protein, and elongation factor 2. Screening conditions were designed based on published conditions for these protein structures or their closely related homologs. From these targeted screenings, we obtained crystals for two proteins, CK-B (Fig. 3B) and LDH that had not emerged from earlier screenings with commercial kits. Both proteins formed three-dimensional crystals from ROS isotonic fractions. Crystals of CK-B diffracted to 1.6 Å, a better resolution than the previously reported structure for bovine creatine kinase (2.3 Å, PDB code: 1G0W) (Tisi, Bax, & Loew, 2001). The structure of CK-B was solved with a human brain-type creatine kinase structure (PDB code: 3B6R) used as the search model (Bong et al., 2008; Fig. 4B); the sequence identity between bovine CK-B and human CK-B was 97%. The structure of CK-B was refined to R_{work} of 22% and R_{free} of 25%. The CK-B crystals belonged to the $P4_3$ space group with unit cells of a = 96 Å, b = 96 Å, c = 107 Å, α = 90°, β = 90°, γ = 90°. Interestingly, proteins extracted from LDH crystals migrated as two close bands on SDS-PAGE gels (Fig. 5). MS analysis indicated that these crystals were composed of LDH chains A and B. Functional LDHs are either homo- (LDHA or LDHB) or heterotetramers (LDH A/B) comprised of either four chains of LDHA or two chains each of LDHA and LDHB, respectively. LDH A/B participates in adjusting LDH levels at different stages of cellular development (Ahmad & Hasnain, 2005). Apparently, LDH crystals obtained from F_G fractions had a heterotetrameric composition, whereas all other available crystal structures of the LDH protein family are in the homotetrameric form. Hence, we were able to capture a unique state of LDH that has never been reported. Figure 5 illustrates the optimization of LDH A/B crystallization from ROS extracts. Initially, LDH A/B crystallized as needles at 4 °C. Although lowering the concentration of polyethylene glycol (PEG 3.5 K) resulted in fewer but longer rod-shaped crystals at RT, these crystals were unstable and degraded within a week. Conditions then were further modified by introducing various salts into the mother liquor. Replacement of $MgSO_4$ with Na-acetate yielded stable pencil-shaped crystals of LDH A/B suitable for diffraction studies. But the diffraction quality for LDH was insufficient to determine the protein's structure.

Crystallization of several proteins with this screening strategy suggests that it can be successfully applied to other designated proteins. Our initial screenings employed commercial protein crystallization kits. Then to obtain protein crystals of specifically targeted proteins, screening conditions were further refined.

3.2. A membrane protein crystallized from ROS membranes

To determine the possibility of crystallizing membrane proteins from ROS membranes, we used opsin as a test model that is expressed at very high levels in these compartments (Palczewski, 2006, 2012). ROS extracts were solubilized with detergent-containing buffer, concentrated, and used directly for protein crystallization. Conditions for crystallization were based on those previously reported for opsin structures (Park, Scheerer, Hofmann, Choe, & Ernst, 2008; Scheerer et al., 2008). Crystals appeared after 1 week of incubation at 4 °C and took about 25 days to achieve their full sizes. X-ray diffraction analysis of these crystals revealed a symmetry consistent with the H3 space group with unit cell dimensions of a = 241.86 Å, b = 241.85 Å, c = 110.45 Å, $\alpha = 90°$, $\beta = 90°$, and $\gamma = 120°$. These diffraction data matched well with those obtained from highly purified opsin crystals (PDB ID: 3CAP). Furthermore, silver staining indicated a molecular weight of ~35 kDa (Fig. 6), which matches the molecular weight of purified opsin and confirms the identity of the crystallized protein as opsin.

3.3. Summary of protein crystallization

Proteins crystallized from ROS had molecular weights ranging from 30 to 50 kDa. Their functions can be classified as phototransduction (arrestin-1 and opsin), glycolysis (GAPDH, enolase, and LDH A/B), and metabolism (CK-B and malate dehydrogenase). Structurally, CK-B existed as a dimer and GAPDH as a tetramer. The other four crystals did not diffract well enough for structural determination or are under optimization. Based on the structures of their related homologs, these proteins are expected to form tetramers in crystals (arrestin-1: PDB code, 1CF1; LDH: PDB code, 1I0Z; enolase: PDB code, 3B97; maltase: PDB code, 1MLD). Therefore, all crystals obtained from ROS were likely oligomeric, a phenomenon similar to that observed for proteins crystallized from *E. coli* (Totir et al., 2012). Table 1 summarizes the crystallization conditions for all proteins crystallized from ROS extracts.

PEGs were the most successful precipitants for crystallization of proteins from ROS extracts, contributing to five out of seven conditions that produced crystals. Most protein crystals were obtained with PEG concentrations between 10% and 20%. For crystals obtained with PEG, the medium molecular weight PEG 3–4 K was the most common, representing 80% of cases. Other conditions with PEGs as major precipitants included 0.1–0.2 *M* salts as coprecipitants. Ammonium sulfate was the second most successful precipitant in these trials. The concentration of ammonium sulfate used for obtaining all crystals ranged between 2 and 3.6 *M*. No crystals were obtained with organic solvents. The most common buffers used were HEPES, Tris, and Na-acetate with a pH range from 5.0 to 8.0.

Protein crystals were obtained at all concentrations above 5 mg/ml for opsin and above 10 mg/ml for all other proteins. Protein crystallization is also affected by the abundance of a

particular protein in heterogeneous samples like ROS extracts. High-abundance proteins crystallize more readily than proteins at low abundance. Hence, crystallization of less abundant proteins (CK-B, LDH A/B, enolase, and maltase) was further enhanced by removing the most abundant proteins from ROS extracts. Thus, removal of GAPDH from the F_B fraction led to the formation of enolase and maltase crystals much more readily during a subsequent screen. Likewise, LDH crystals formed following the removal of arrestin-1 from the F_C fraction.

In total, crystals of seven different proteins were obtained from ROS isotonic fractions with maximum resolutions ranging from 1.6 to 20 Å (data not shown). Some crystals were detected in about one week, whereas others took longer. Among these proteins, structures were previously reported for CK-B (PDB code: 1G0W) [26], opsin (PDB code: 3CAP) [29], and arrestin-1 (PDB code: 1CF1) (Fig. 3C) [30]. Structures of GAPDH, LDH, enolase, and maltase from a bovine source have yet to be published.

3.4. Reproducibility

Crystallization occurs as a result of random association events influenced by several factors. ROS extracts were comprised of a mixture of various proteins, making it essential to assess the reproducibility of crystallization. For hits obtained from initial screens, the basic conditions were repeated and optimized to obtain crystals for further studies. Even though the morphology and size of the crystals responded to the changes in type and concentration of precipitants employed, crystallization of all proteins discussed in this study appeared to be reproducible.

4. CONCLUSIONS

Here, we investigated the crystallization profile of crude extracts from bovine ROS. In total, seven proteins were crystallized among which three formed diffraction-quality crystals after a series of crystallization condition optimizations. Structures are reported here for two of these proteins (bovine GAPDH and CK-B).

Successful crystallization of multiple proteins from complex ROS extracts indicates that many proteins from mammals also have high propensity to crystallize. Among the studied proteins, GAPDH ranked first with respect to its tendency to crystallize from ROS extracts. Arrestin was next, crystallizing under many different conditions. Although some proteins formed poorly diffracting crystals, LDH crystals featured a heterologous tetrameric composition, whereas all the other available structures for this protein family were homotetramers. Thus, we captured an unreported, naturally occurring oligomeric state of LDH. Furthermore, crystallization of opsin from ROS extracts validates the use of crude ROS membranes or heterogeneous sample preparations for initial crystallization screening of highly abundant membrane proteins. This would facilitate the identification of crystallization hits for such proteins and markedly reduce the time and expense involved in testing multiple crystallization conditions.

The tendency of mammalian proteins to crystallize has other implications. Traditionally, proteins are separated from their native environment and purified to homogeneity before

crystallization. Our findings regarding the intrinsic crystallization propensity of mammalian proteins open a new avenue to conduct structural studies on native-source proteins, circumventing the need for exhausting purification and further downstream processing. Methodology used in this study is easily scalable for structural studies of proteomes from other tissues and organisms. It could also be especially helpful for protein complexes that are not well expressed in heterologous systems. Another major advantage of using complex rather than purified protein samples is that the former retain proteins and their complexes in their native states, and hence increase their likelihood of crystallizing in an unperturbed manner.

Even though the methods used in this study are biased toward proteins with a high tendency to crystallize, such proteins could serve as crystallization-inducers by cocrystallizing along with a targeted binding partner. An interesting avenue for future studies would be to explore the feasibility of using native-source proteins for structural studies of protein–protein interactions and other complex biological events.

ACKNOWLEDGMENTS

We thank Drs. Leslie T. Webster, Jr., Marcin Golczak, and Yaroslav Tsybovsky (Case Western Reserve University, CWRU) for their comments on the manuscript, Dr. Narayanasami Sukumar helped with the data collection on the native form of GAPDH at NE-CAT/Cornell University. We thank Dr. Philip Kiser for helping with synchrotron data collection, Dr. Beata Jastrzebska for her long-time support on PDE6 preparation, Susan Farr and Satsumi Roos for helping with ROS preparations. We also thank The Protein Expression Purification Crystallization Core at Case Western Reserve University for use of their equipment and Summer J. Watterson for her help. This study was inspired by the RPE65 crystallization experiment, Kiser, Golczak, Lodowski, Chance, & Palczewski. (2009). The work was supported by funding from the National Eye Institute, National Institutes of Health Grants R24EY021126 (to K. P.), R01EY008061 (to K. P.). K. P. is John H. Hord Professor of Pharmacology.

This publication was made possible by the Center for Synchrotron Biosciences Grant, P30-EB-00998, in support of beamline X29 from the National Institute of Biomedical Imaging and Bioengineering. The work is also based upon research conducted at the Advanced Photon Source on the Northeastern Collaborative Access Team beamlines, which are supported by a grant from the National Institute of General Medical Sciences (P41 GM103403) from the National Institutes of Health. Use of the Advanced Photon Source, an Office of Science User Facility operated for the U.S. Department of Energy (DOE) Office of Science by Argonne National Laboratory, was supported by the U.S. DOE under Contract No. DE-AC02-06CH11357.

ABBREVIATIONS

CK-B	creatine kinase-B type
DEAE	diethylaminoethyl
GAPDH	glyceraldehyde 3-phosphate dehydrogenase
G_t	transducin (rod-specific G protein)
HEPES	2-[4-(2-hydroxyethyl)piperazin-1-yl]ethanesulfonic acid
LDH	L-lactate dehydrogenase
MS	mass spectroscopy
NAD	nicotinamide adenine dinucleotide
PDE6	phosphodiesterase 6

PEG	polyethylene glycol
ROS	rod outer segment(s)

REFERENCES

Ahmad R, Hasnain AU. Ontogenetic changes and developmental adjustments in lactate dehydrogenase isozymes of an obligate air-breathing fish Channa punctatus during deprivation of air access. Comparative Biochemistry and Physiology. Part B, Biochemistry & Molecular Biology. 2005; 140(2):271–278. http://dx.doi.org/10.1016/j.cbpc.2004.10.012.

Baker BY, Palczewski K. Detergents stabilize the conformation of phosphodiesterase 6. Biochemistry. 2011; 50(44):9520–9531. http://dx.doi.org/10.1021/bi2014695. [PubMed: 21978030]

Baker BY, Shi W, Wang B, Palczewski K. High-resolution crystal structures of the photoreceptor glyceraldehyde 3-phosphate dehydrogenase (GAPDH) with three and four-bound NAD molecules. Protein Science. 2014; 23(11):1629–1639. doi.10.1002/pro.2543. Epub 2014 Sep 25. [PubMed: 25176140]

Bong SM, Moon JH, Nam KH, Lee KS, Chi YM, Hwang KY. Structural studies of human brain-type creatine kinase complexed with the ADP-Mg^{2+}-NO_3^--creatine transition-state analogue complex. FEBS Letters. 2008; 582(28):3959–3965. http://dx.doi.org/10.1016/j.febslet.2008.10.039. [PubMed: 18977227]

Buczylko J, Palczewski K. Purification of arrestin from bovine retinas. Methods in Neurosciences. 1993; 15:226–236.

Cowan-Jacob SW, Kaufmann M, Anselmo AN, Stark W, Grutter MG. Structure of rabbit-muscle glyceraldehyde-3-phosphate dehydrogenase. Acta Crystallographica. Section D, Biological Crystallography. 2003; 59(Pt. 12):2218–2227.

Dong A, Xu X, Edwards AM, Midwest Center for Structural Genomics; Structural Genomics Consortium. Chang C, et al. In situ proteolysis for protein crystallization and structure determination. Nature Methods. 2007; 4(12):1019–1021. http://dx.doi.org/10.1038/nmeth1118. [PubMed: 17982461]

Emsley P, Lohkamp B, Scott WG, Cowtan K. Features and development of Coot. Acta Crystallographica. Section D, Biological Crystallography. 2010; 66(Pt. 4):486–501. http://dx.doi.org/10.1107/S0907444910007493.

Fischer EH, Krebs EG. The isolation and crystallization of rabbit skeletal muscle phosphorylase b. The Journal of Biological Chemistry. 1958; 231(1):65–71. [PubMed: 13538948]

Goc A, Angel TE, Jastrzebska B, Wang B, Wintrode PL, Palczewski K. Different properties of the native and reconstituted heterotrimeric G protein transducin. Biochemistry. 2008; 47(47):12409–12419. http://dx.doi.org/10.1021/bi8015444. [PubMed: 18975915]

Goddard TD, Huang CC, Ferrin TE. Visualizing density maps with UCSF Chimera. Journal of Structural Biology. 2007; 157(1):281–287. http://dx.doi.org/10.1016/j.jsb.2006.06.010. [PubMed: 16963278]

Jenkins JL, Tanner JJ. High-resolution structure of human D-glyceraldehyde-3-phosphate dehydrogenase. Acta Crystallographica. Section D, Biological Crystallography. 2006; 62(Pt. 3):290–301. http://dx.doi.org/10.1107/S0907444905042289.

Judge RA, Forsythe EL, Pusey ML. The effect of protein impurities on lysozyme crystal growth. Biotechnology and Bioengineering. 1998; 59(6):776–785. [PubMed: 10099398]

Kabsch W. Integration, scaling, space-group assignment and post-refinement. Acta Crystallographica. Section D, Biological Crystallography. 2010a; 66(Pt. 2):133–144. http://dx.doi.org/10.1107/S0907444909047374.

Kabsch W. XDS. Acta Crystallographica. Section D, Biological Crystallography. 2010b; 66(Pt. 2):125–132. http://dx.doi.org/10.1107/S0907444909047337.

Kim YJ, Hofmann KP, Ernst OP, Scheerer P, Choe HW, Sommer ME. Crystal structure of pre-activated arrestin p44. Nature. 2013; 497(7447):142–146. http://dx.doi.org/10.1038/nature12133. [PubMed: 23604253]

Kiser PD, Golczak M, Lodowski DT, Chance MR, Palczewski K. Crystal structure of native RPE65, the retinoid isomerase of the visual cycle. Proceedings of the National Academy of Sciences of the United States of America. 2009; 106(41):17325–17330. http://dx.doi.org/10.1073/pnas.0906600106, 0906600106 [pii]. [PubMed: 19805034]

Kors CA, Wallace E, Davies DR, Li L, Laible PD, Nollert P. Effects of impurities on membrane-protein crystallization in different systems. Acta Crystallographica. Section D, Biological Crystallography. 2009; 65(Pt. 10):1062–1073. http://dx.doi.org/10.1107/S0907444909029163, S0907444909029163 [pii].

Kwok MC, Holopainen JM, Molday LL, Foster LJ, Molday RS. Proteomics of photoreceptor outer segments identifies a subset of SNARE and Rab proteins implicated in membrane vesicle trafficking and fusion. Molecular & Cellular Proteomics. 2008; 7(6):1053–1066. http://dx.doi.org/10.1074/mcp.M700571-MCP200. [PubMed: 18245078]

Mcpherson A. A brief-history of protein crystal-growth. Journal of Crystal Growth. 1991; 110(1–2):1–10. http://dx.doi.org/10.1016/0022-0248(91)90859-4.

Muller DJ, Wu N, Palczewski K. Vertebrate membrane proteins: Structure, function, and insights from biophysical approaches. Pharmacological Reviews. 2008; 60(1):43–78. http://dx.doi.org/10.1124/pr.107.07111, pr.107.07111 [pii]. [PubMed: 18321962]

Otwinowski Z, Minor W. Processing of X-ray diffraction data collected in oscillation mode. Macromolecular Crystallography, Part A. 1997; 276:307–326. http://dx.doi.org/10.1016/S0076-6879(97)76066-X.

Palczewski K. G protein-coupled receptor rhodopsin. Annual Review of Biochemistry. 2006; 75:743–767. http://dx.doi.org/10.1146/annurev.biochem.75.103004.142743.

Palczewski K. Chemistry and biology of vision. The Journal of Biological Chemistry. 2012; 287(3):1612–1619. http://dx.doi.org/10.1074/jbc.R111.301150. [PubMed: 22074921]

Park JH, Scheerer P, Hofmann KP, Choe HW, Ernst OP. Crystal structure of the ligand-free G-protein-coupled receptor opsin. Nature. 2008; 454(7201):183–187. http://dx.doi.org/10.1038/nature07063, nature07063 [pii]. [PubMed: 18563085]

Pettersen EF, Goddard TD, Huang CC, Couch GS, Greenblatt DM, Meng EC, et al. UCSF Chimera–a visualization system for exploratory research and analysis. Journal of Computational Chemistry. 2004; 25(13):1605–1612. http://dx.doi.org/10.1002/jcc.20084. [PubMed: 15264254]

Pettigrew GW, Bartsch RG, Meyer TE, Kamen MD. Redox potentials of photosynthetic bacterial cytochromes-C2 and structural bases for variability. Biochimica et Biophysica Acta. 1978; 503(3):509–523. http://dx.doi.org/10.1016/0005-2728(78)90150-0. [PubMed: 28760]

Sachs K, Maretzki D, Hofmann KP. Assays for activation of opsin by all-trans-retinal. Methods in Enzymology. 2000; 315:238–251. [PubMed: 10736706]

Scheerer P, Park JH, Hildebrand PW, Kim YJ, Krauss N, Choe HW, et al. Crystal structure of opsin in its G-protein-interacting conformation. Nature. 2008; 455(7212):497–502. http://dx.doi.org/10.1038/nature07330, nature07330 [pii]. [PubMed: 18818650]

Skiba NP, Spencer WJ, Salinas RY, Lieu EC, Thompson JW, Arshavsky VY. Proteomic identification of unique photoreceptor disc components reveals the presence of PRCD, a protein linked to retinal degeneration. Journal of Proteome Research. 2013; 12(6):3010–3018. http://dx.doi.org/10.1021/pr4003678. [PubMed: 23672200]

Tisi D, Bax B, Loew A. The three-dimensional structure of cytosolic bovine retinal creatine kinase. Acta Crystallographica. Section D, Biological Crystallography. 2001; 57(Pt. 2):187–193.

Totir M, Echols N, Nanao M, Gee CL, Moskaleva A, Gradia S, et al. Macro-to-micro structural proteomics: Native source proteins for high-throughput crystallization. PLoS One. 2012; 7(2):e32498. http://dx.doi.org/10.1371/journal.pone.0032498. [PubMed: 22393408]

Vagin AA, Steiner RA, Lebedev AA, Potterton L, McNicholas S, Long F, et al. REFMAC5 dictionary: Organization of prior chemical knowledge and guidelines for its use. Acta Crystallographica. Section D, Biological Crystallography. 2004; 60(Pt. 12 Pt. 1):2184–2195. http://dx.doi.org/10.1107/S0907444904023510.

Winn MD, Ballard CC, Cowtan KD, Dodson EJ, Emsley P, Evans PR, et al. Overview of the CCP4 suite and current developments. Acta Crystallographica. Section D, Biological Crystallography. 2011; 67(Pt. 4):235–242. http://dx.doi.org/10.1107/S0907444910045749.

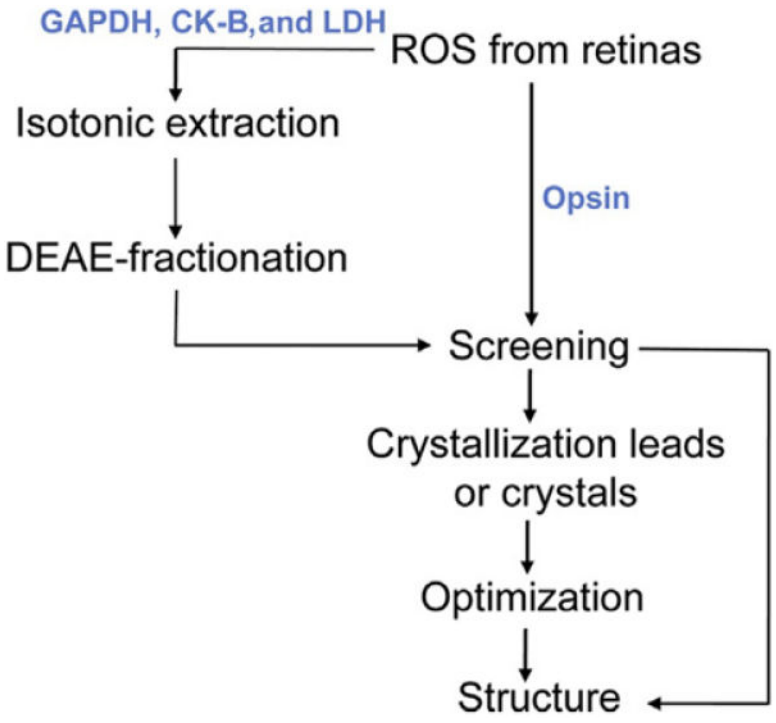

Figure 1.

Flowchart illustrating the protocol used for crystallizing proteins from bovine ROS. Isotonic extraction and DEAE-ion-exchange chromatography were employed for fractionating all proteins from bovine ROS except opsin.

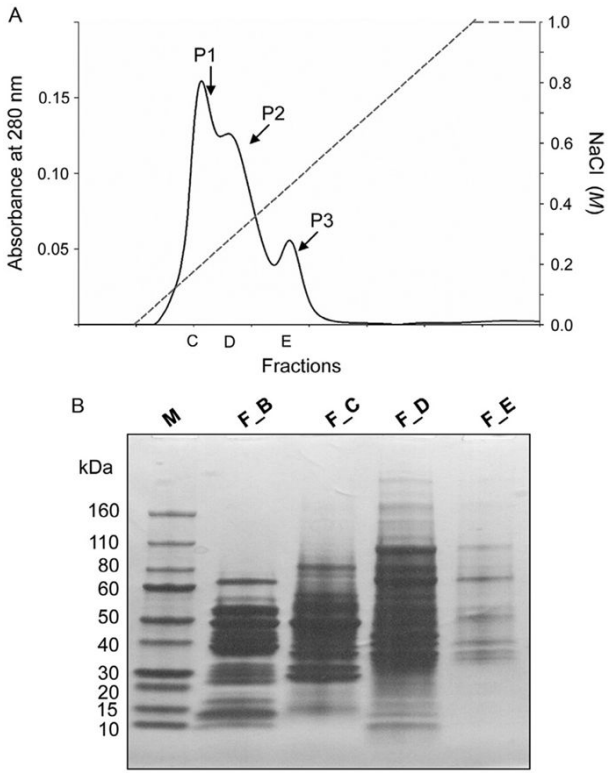

Figure 2.

Protein sample preparation from bovine ROS. (A) Proteins from ROS isotonic extracts were fractionated by DEAE-ion-exchange chromatography. In a typical preparation, proteins eluted from the column in three major peaks. (B) Fractions corresponding to the three major elution peaks (P1, P2, and P3) were collected along with the flow-through (F). The protein composition of each peak was checked by SDS-PAGE with M indicating the molecular marker lane. F_B: flow-through; F_C: elution peak 1; F_D: elution peak 2; F_E: elution peak 3.

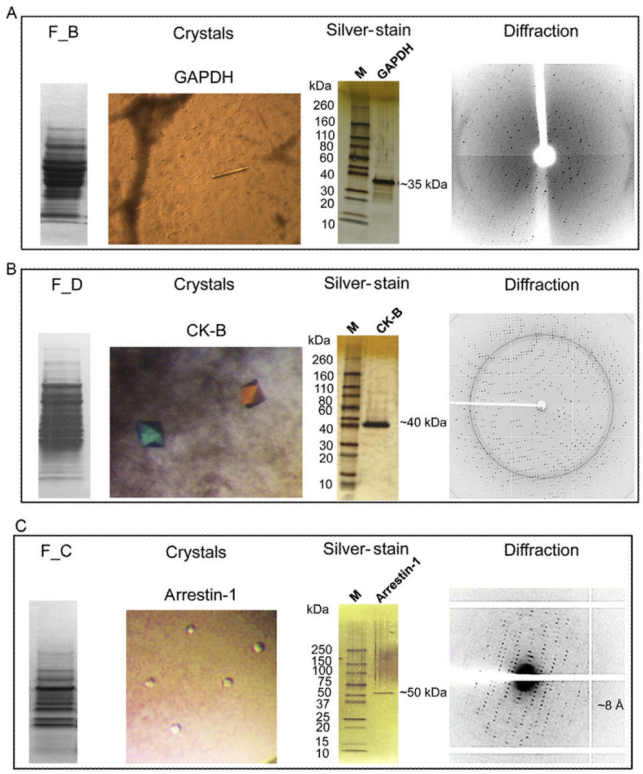

Figure 3.

Three examples of crystallization of proteins from complex samples. Single crystals were examined by a silver-stained gel readout and a diffraction test. (A) Study of GAPDH showing rod-shaped crystals. (B) Study of CK-B exhibiting triclinic crystals. (C) Study of arrestin-1 revealing cubic crystals. F_B indicates the DEAE-cellulose flow-through fraction, F_C designates the DEAE-cellulose peak 1 fraction and F_D corresponds to the DEAE-cellulose peak 2 fraction.

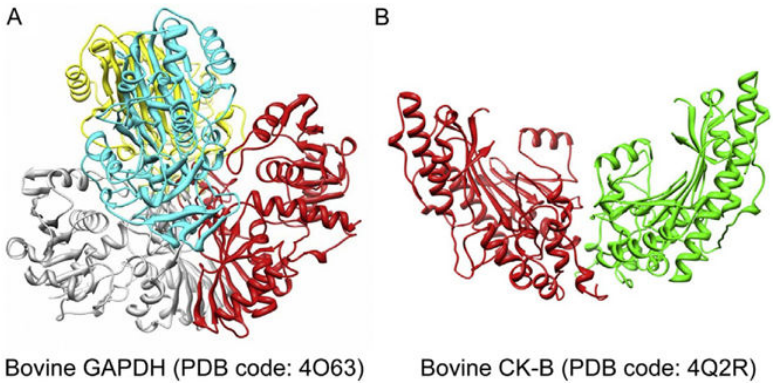

Figure 4.

Ribbon representations of bovine GAPDH (left panel) solved to 1.93 Å and bovine CK-B (right panel) solved to 1.65 Å. Individual subunits are presented in different colors.

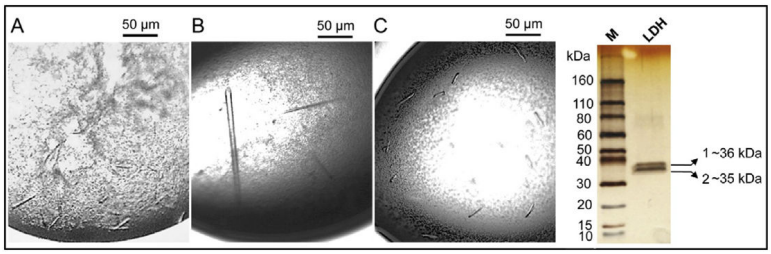

Figure 5.

Optimization of LDH crystallization conditions. (A) LDH initially formed crystalline needles at 4 °C. (B) By lowering the PEG concentration, fewer and longer rod crystals were obtained at room temperature. (C) Replacement of $MgSO_4$ with 0.2 *M* Na-acetate yielded stable pencil-shaped crystals suitable for diffraction studies. Size bars of 50 μm are shown at the top of the crystal images. (D) Silver-staining analysis of a single LDH crystal revealed two distinguishable bands on a SDS-PAGE gel.

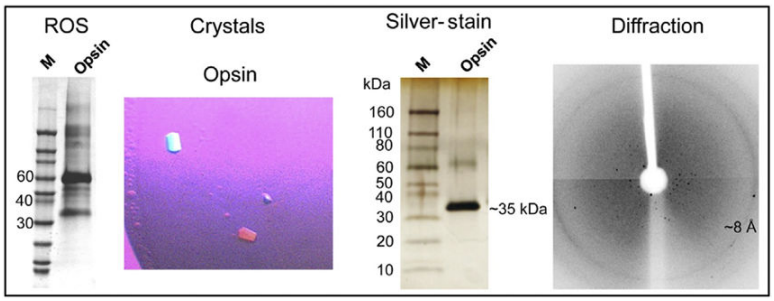

Figure 6.

Opsin crystallization from bovine ROS. Hexagonal crystals (~90 μm in their longest dimension) were obtained from photobleached ROS membranes. Crystals were characterized by silver staining and X-ray diffraction. The outermost reflections correspond to 8 Å.

Table 1

Protein crystals from bovine ROS

Crystal number	ROS fractiona[a]	MW (kDa)	Protein identification	Crystallization conditions	Diffraction (Å)	Structure type
#1	F_A and F_B	36	Glyceraldehyde-3-phosphate dehydrogenase	20% PEG 3.5 K; 0.2 *M* succinic acid, pH 7.0	1.9	Homotetramer
#2	F_D	42	Creatine kinase-B type	1.8 *M* ammonium sulfate; 0.1 *M* HEPES, pH 7.5; 3% PEG 1 K	1.6	Dimer
#3	F_G	36	L-Lactate dehydrogenase A and B chain	10% PEG 3.5 K; 0.2 *M* Na-acetate	10	Under optimization
#4	F_C	45	S-Antigen (arrestin-1)	7.5% PEG 3.5 K; 0.1 *M* Na-malonate, pH 5.0; 4% PEG 400	6	Under optimization
#5	F_F	36	Malate dehydrogenase	25% PEG 1 K; 0.1 *M* Na/K-phosphate, pH 6.5; 0.2 *M* NaCl	8	Under optimization
#6	F_F	47	α-Enolase	20% PEG 3.5 K; 0.2 *M* Na-thiocyanate	20	Under optimization
#7	ROS	35	Opsin	3.0–3.6 *M* ammonium sulfate; 0.1 *M* Na-acetate, pH 5.6	8	Under optimization

[a]F_A: ROS isotonic extraction. F_B: ROS isotonic extraction/DEAE-cellulose flow-through. F_C: ROS isotonic extraction/DEAE-cellulose, peak 1. F_D: ROS isotonic extraction/DEAE-cellulose, peak 2. F_F: ROS isotonic extraction/DEAE-cellulose, flow/NAD-flow. F_G: ROS isotonic extraction/DEAE-cellulose, peak 1/Heparin-flow.